



OPEN

A multi-parameter tunable plasmon modulator

Xuefang Hu^{1,2✉}, Changgui Lu³, Xiangyue Zhao³, Yinwei Gu³, Mengjia Lu³ & Dechao Sun¹

Multi-parameter control of light is a key functionality to modulate optical signals in photonic integrated circuits for various applications. However, the traditional optical modulators can only control one or two properties of light at the same time. Herein, we propose a hybrid structure which can modulate the amplitude, wavelength and phase of surface plasmon polaritons (SPPs) simultaneously to overcome these limitations. The numerical results show that when the Fermi level of graphene changes from 0.3 to 0.9 eV, the variation of optical transmission, wavelength and phase are 32.7 dB, 428 nm and 306°, respectively. The demonstrated structure triggers an approach for the realization of ultracompact modulation and has potential applications in the fields of optical switches, communications and photo-detection.

As the essential property of electromagnetic field, polarization, wavelength, amplitude and phase reflect a wealth of applications in optical perception and operation^{1–4}. Effectively manipulating of these parameters at micro/nanoscales is of great significance and has been widely exploited in optical communication^{5–8}, optical sensing^{9–11}, photo-detection^{7,12} and so on. Surface plasmon polaritons (SPPs), originating from the interaction between free electrons of metal and the electromagnetic waves, hold a more potential applications at micro/nanoscales because they can break the conventional diffraction limit^{13,14}. Herein, the active control of SPPs has attracted great attention of researchers^{15,16}.

Currently, much work has been done in multi-parameter modulation to meet the increasing demand for various application scenarios^{17–19}. For example, Zhuang Ren's group demonstrated an active and smart electro-optic THz modulator, which is based on a strongly correlated electron oxide vanadium dioxide (VO₂). With milliamperic current excitation on the VO₂ thin film, the transmission, reflection, absorption and phase of THz waves can be modulated efficiently. In particular, the antireflection condition can be actively achieved and the modulation depth reaches 99.9%, accompanied by a 180° phase switching²⁰. Ali Forouzmard's group proposed an electrically tunable amplitude and phase modulators, which are designed by the hybridization of indium tin oxide (ITO) into a guided-mode resonance mirror. A gate-tunable amplitude modulator with a modulation depth as high as ~ 0.80 is realized, and the phase variation of ~ 210° is accomplished when the applied bias voltage alters from – 15 V to + 24 V²¹. However, these proposed modulators can only control one or two parameter of light despite its superior performance, which greatly hinders their widely application^{22,23}. Herein, a modulator which can control more properties of light will attract much attention of experts.

In this paper, a hybrid silicon-dielectric-graphene-grating structure is proposed, which can modulate the amplitude, wavelength and phase of SPPs simultaneously. The SPPs is stimulated by the grating and propagating on the graphene, the Fermi level of the graphene is controlled by the voltage applied between silicon substrate and graphene. The numerical results show that when the Fermi level changes from 0.3 to 0.9 eV, the variation of optical transmission, wavelength and phase are 32.7 dB, 428 nm and 306°, respectively. This structure has the potential application in the fields of optical switches, communications and photo-detection^{24,25}.

Model and analysis

In Fig. 1, we illustrate the three-dimensional (3D) schematic diagram of our designed hybrid silicon-dielectric-graphene-grating structure. A TM polarized light incidents on the gold grating and excites the SPPs propagating along the graphene surface. The Fermi level of the graphene is controlled by the voltage applied between silicon substrate and the graphene, leading to the amplitude, wavelength and phase of SPPs modulated simultaneously. Because the calcium fluoride (CaF₂) exhibit an excellent performance such as low leakage current, high dielectric strength and low amounts of defects, we select the CaF₂ as the dielectric layer, which could improve the performance of modulator effectively²⁶.

¹College of Digital Technology and Engineering, Ningbo University of Finance & Economics, Ningbo 315175, Zhejiang, China. ²Key Laboratory of Optical Information Detection and Display Technology of Zhejiang, Zhejiang Normal University, Jinhua 321004, Zhejiang, China. ³Advanced Photonics Center, School of Electronic Science and Engineering, Southeast University, Nanjing 210096, Jiangsu, China. ✉email: huxuefang@nbufe.edu.cn

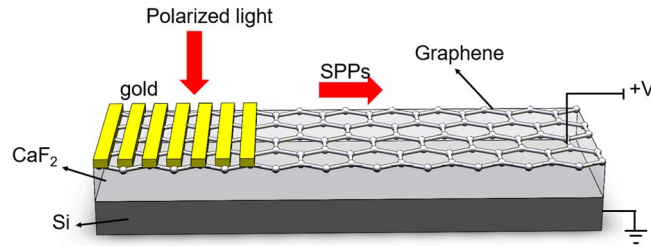


Figure 1. 3D Schematic diagram of silicon-dielectric-graphene-grating structure. The polarized light incident on the gold grating and excites the SPPs propagating along the graphene surface. The Fermi level of the graphene is controlled by the voltage applied between silicon substrate and the graphene.

To understand the relationship between the applied voltage and the carrier density in our model, a theoretical relationship between them is shown in Eq. (1), where ϵ , ϵ_0 and ϵ_r are the charge constant, the permittivity of vacuum and the relative permittivity of CaF_2 respectively, V and d are the voltage and thickness of CaF_2 . The relation between Fermi level and the carrier density is presented in Eq. (2), where \hbar , V_f and n_g are the reduced Planck constant, Fermi velocity and carrier density respectively, where $V_f = 10^6$ m/s^{27–29}. Herein, the Fermi level of the graphene can be modulated by the voltage effectively and dynamically^{30,31}.

$$n_g = \frac{\epsilon_0 \epsilon_r V}{ed}, \tag{1}$$

$$E_f = \hbar V_f \sqrt{\pi n_g}. \tag{2}$$

The proposed structure is simulated with the finite element method (FEM), and the two-dimensional (2D) simulation model is shown in Fig. 2. The port mode is used to excite the SPPs, (The grating is just used to excite the SPPs, so it is unnecessary to take the grating into consideration in simulation since the excitation efficiency is insignificant here and other excitation method can be applied.) and then the characteristics of the SPPs are analyzed by changing the Fermi level of graphene (The details about the simulation are shown in section of method). Firstly, the electric field distribution and optical transmittance are used to reflect the modulation about the amplitude. Secondly, the change in wavelength can be observed in the distribution of electric field too. Finally, the phase distribution of this model is presented. Thus, the demonstrated simulation model can vividly reflect the modulation about the amplitude, wavelength and phase.

For the model of anisotropic graphene, its out-of-plane permittivity is set to 2.5, and the in-plane conductivity can be obtained from random-phase approximation, including the effect of finite temperature ($T = 300$ K):

$$\sigma_g = \frac{2ie^2 K_B T}{\pi \hbar^2 (\omega + i\tau^{-1})} \text{In} \left[2 \cosh \left(\frac{E_f}{2K_B T} \right) \right] + \frac{e^2}{4\pi \hbar} \left\{ -\frac{i}{2} \text{In} \frac{(\hbar\omega + 2E_f)^2}{(\hbar\omega - 2E_f) + (2K_B T)^2} + \frac{\pi}{2} + \arctan \left(\frac{\hbar\omega - 2E_f}{2K_B T} \right) \right\}. \tag{3}$$

Here σ_g and k_B are the conductivity of graphene and the Boltzmann's constant. E_f and ω are the Fermi energy level and radian frequency, respectively. The carrier relaxation time $\tau = \mu E_f / ev_f^2$, where the Fermi velocity $v_f = 10^6$ m/s and carrier mobility $\mu = 10,000$ $\text{cm}^2/(\text{V s})$. The effective permittivity of graphene ϵ_g can be described by means of the following expression:

$$\epsilon_g = 1 + \frac{i\sigma_g}{\omega \epsilon_0 t_g}, \tag{4}$$

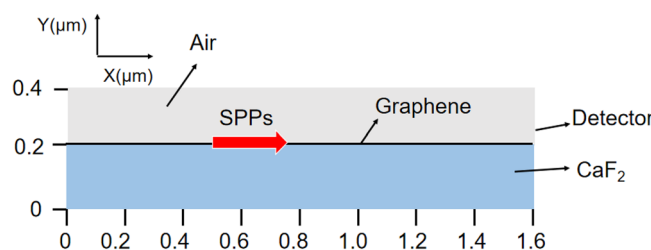


Figure 2. 2D simulation model of proposed hybrid silicon-dielectric-graphene-grating structure, the port mode is used to excite the SPPs.

where ϵ_0 and $t_g = 0.33$ nm represent the vacuum permittivity and thickness of graphene respectively²⁷.

Results and discussion

Amplitude. Figure 3 depicts the y component of electric field at different Fermi levels, and the working wavelength is fixed at 8 μm . Figure 3a is the y component of the electric field when the Fermi level is 0.4 eV. The distribution of electric field is the typical SPPs and just presents a normal attenuation. The y component of the electric field is drawn in Fig. 3b when the Fermi level is 0.6 eV as the voltage increases. It can be obtained that the strength of the electric field is enhanced and the loss of SPPs is decreased, resulting in a longer SPPs propagating distance. In addition, the wavelength of propagating SPPs is also increased. The y component of the electric field when the Fermi level is 0.8 eV is shown in Fig. 3c, and the change in amplitude and the wavelength is more obvious. The distribution of electric field at different Fermi level proves that the proposed silicon-dielectric-graphene-grating structure can control the amplitude and the wavelength of SPPs effectively via changing the applied voltage.

Figure 4 shows the relationship between electric intensity and the Fermi levels of graphene. It can be seen that the electric intensity of fourth peak at the Fermi level of 0.4 eV is 1.24×10^5 V/m, while it is 1.37×10^5 V/m when the Fermi level increases to 0.6 eV. The electric field intensity reaches 1.53×10^5 V/m as the Fermi level increases to 0.8 eV, and it has changed about 23.3%. It can be concluded that with the increase of the Fermi level, the amplitude of the SPPs increases gradually.

Figure 5 shows the relationship between optical transmittance and different Fermi levels of graphene. It can be obtained that the optical transmission increases obviously as the Fermi level increases, because the propagation losses is decreased owing to the increase of carrier density. The optical transmission changes about 32.7 dB (-47 dB at 0.3 eV while -13.3 dB at 0.8 eV). It further illustrates that our proposed structure can effectively control the amplitude of the propagating SPPs dynamically by changing the Fermi level of graphene.

The wavelength. Figure 6 is the relationship between wavelength of SPPs and the Fermi levels of graphene. It can be obtained from picture that the wavelength of the propagating SPPs increases when the Fermi level increases, owing to the wavelength of graphene plasmon that is in direct proportional to the Fermi level of the graphene³². The wavelength changes by 428 nm when the Fermi level of graphene increase from 0.3 to 0.9 eV (226 nm at 0.3 eV while 654 nm at 0.9 eV). The results verify that the wavelength of the SPPs can also be modulated by the demonstrated structure effectively.

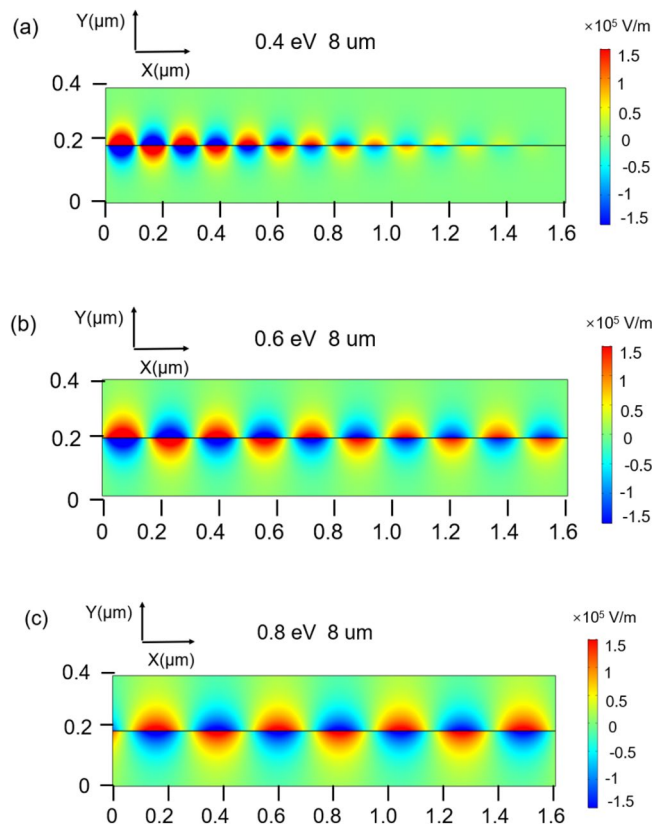


Figure 3. The y component of electric field distribution when the Fermi level of graphene is (a) 0.4 eV (b) 0.6 eV (c) 0.8 eV.

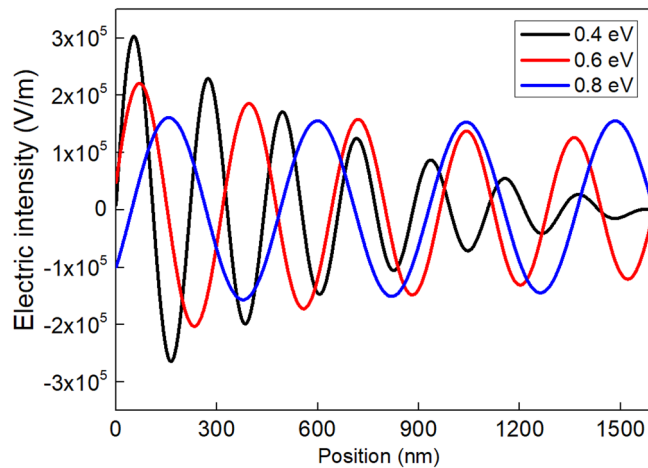


Figure 4. The relationship between electric intensity and Fermi levels of graphene.

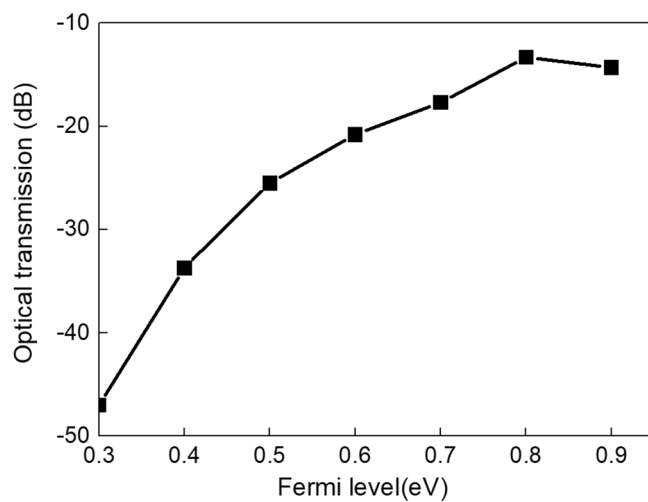


Figure 5. The relationship between optical transmission and the Fermi levels of graphene.

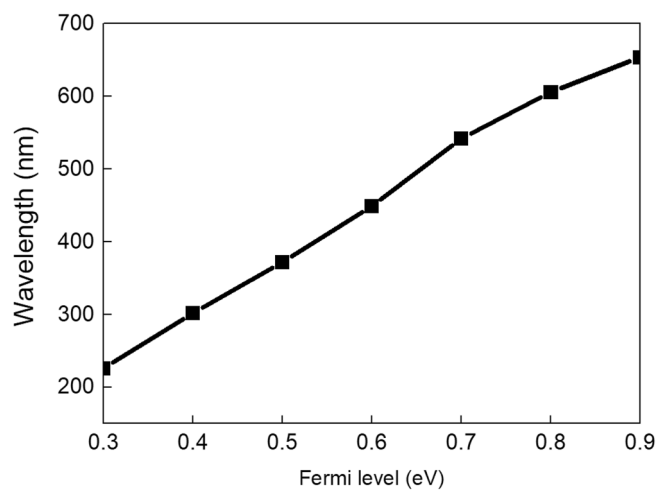


Figure 6. The relationship between wavelengths of SPPs and Fermi levels.

The phase. Figure 7 shows the x component of the phase distribution when the graphene is of different Fermi levels. It can be clearly seen that the phase present various distribution for different Fermi levels, which verifies that our proposed structure can also be utilized to control the phase of SPPs dynamically.

The phase of SPPs can be affected by both the refractive index and the propagation length of graphene due to the change of optical path. Figure 8 is the relationship between the phase at the right port and the Fermi levels of graphene when the propagation length d is 1.6 μm and 1.8 μm , respectively (the operating wavelength is fixed at 8 μm). The phase is -139° when the Fermi level of graphene is 0.3 eV, and the phase is 167° when the Fermi level increases to 0.5 eV at the propagation length of 1.6 μm . The phase changes at right port changes can reach to 306° . (While the phase is 145° when the Fermi level of graphene is 0.3 eV, and the phase is -154° when the Fermi level increases to 0.9 eV at the propagation length of 1.8 μm . The phase changes 299°). Thus, the amplitude,

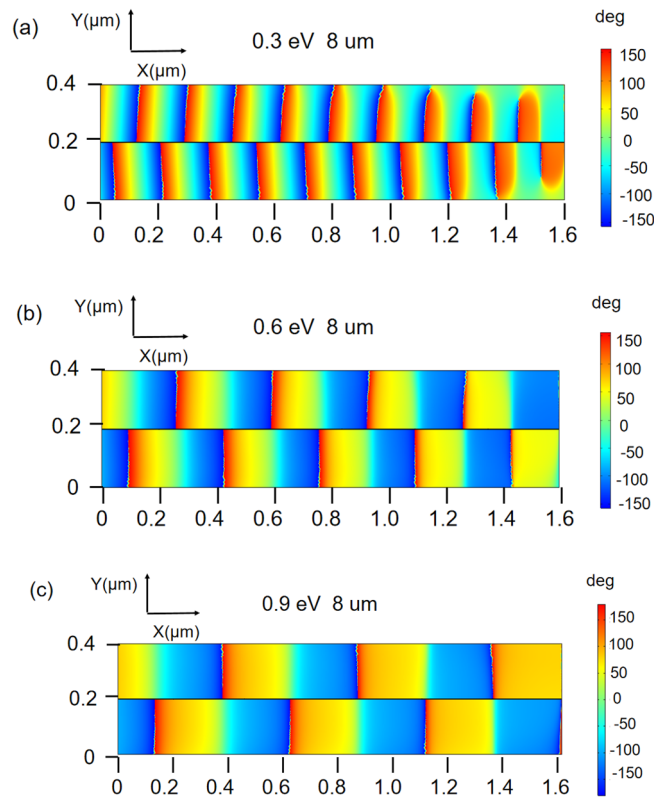


Figure 7. The phase distribution at different Fermi levels (a) 0.4 eV (b) 0.6 eV (c) 0.9 eV.

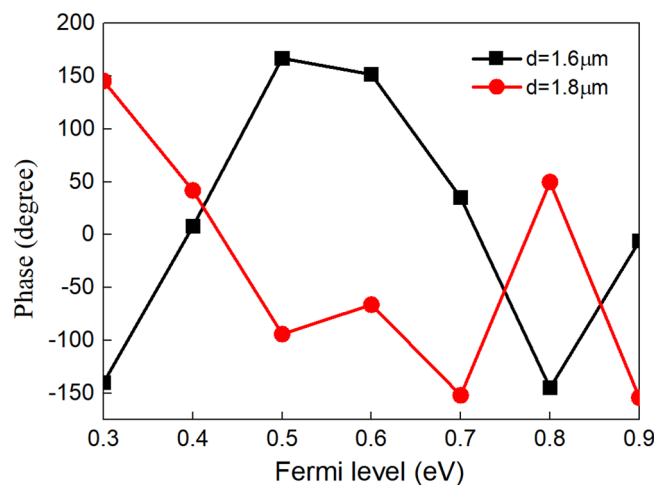


Figure 8. The relationship between phase at right port and the Fermi levels of graphene when the propagation lengths are 1.6 μm and 1.8 μm , respectively.

wavelength and phase of propagating SPPs in our model can be simultaneously controlled through the Fermi level of graphene by changing the applied voltage, which will have a potential application in modern integrated optics and communication³³.

Conclusion

In conclusion, we have demonstrated a silicon-dielectric-graphene-grating hybrid structure. The amplitude, wavelength and phase of SPPs can be modulated simultaneously when the SPPs is propagating along the graphene. The numerical results show that when the Fermi level of graphene changes from 0.3 to 0.9 eV, the optical transmission, wavelength and phase are changed by 32.7 dB, 428 nm and 306°, respectively. The realization of multi-parameter modulation in SPPs will have a promising application in the field of optical communication, sensor and photo-detection.

Methods

The simulation has been performed using the commercial finite element method (FEM), trial version of software “COMSOL Multiphysics 5.5”. In simulation, the scattering boundary condition and user-defined port are used. The module of radio frequency is used to investigate the relationship between voltage and optical transmission, wavelength and phase. The surface conductivity model and the transitional boundary condition are used in the model of graphene. In addition, the permittivity of CaF₂ is set as 6.76. The mesh size is 1/5 of one wavelength.

Data availability

The data relative to the experiments discussed in this work are available upon reasonable request from the corresponding author Xuefang Hu.

Received: 12 December 2022; Accepted: 14 July 2023

Published online: 17 July 2023

References

- Liu, M. *et al.* A graphene-based broadband optical modulator. *Nature* **474**(7349), 64–67 (2011).
- Melikyan, A. *et al.* High-speed plasmonic phase modulators. *Nat. Photon.* **8**, 229–233 (2014).
- Wei, H. *et al.* Cascaded logic gates in nanophotonic plasmon networks. *Nat. Commun.* **2**, 387 (2011).
- Zhu, L. *et al.* Electrical control of terahertz polarization by graphene microstructure. *Opt. Commun.* **346**, 120–123 (2015).
- Thijssen, R. *et al.* Plasmon nanomechanical coupling for nanoscale transduction. *Nano Lett.* **13**, 3293–3297 (2013).
- Schuller, J. A. *et al.* Plasmonics for extreme light concentration and manipulation. *Nat. Mater.* **9**(3), 193–204 (2010).
- Sorger, V. J. *et al.* Experimental demonstration of low-loss optical waveguiding at deep sub-wavelength scales. *Nat. Commun.* **2**(1), 1–5 (2011).
- Ozbay, E. Plasmonics: Merging photonics and electronics at nanoscale dimensions. *Science* **311**(5758), 189–193 (2006).
- Rodrigo, D. *et al.* Mid-infrared plasmonic biosensing with graphene. *Science* **349**(6244), 165–168 (2015).
- Bareza, N. J. *et al.* Mid-infrared gas sensing using graphene plasmons tuned by reversible chemical doping. *ACS Photonics* **7**(4), 879–884 (2020).
- Liu, Z. *et al.* Focusing surface plasmons with a plasmonic lens. *Nano Lett.* **5**(9), 1726–1729 (2005).
- Brar, V. W. *et al.* Electronic modulation of infrared radiation in graphene plasmonic resonators. *Nat. Commun.* **6**(1), 1–7 (2015).
- Luxmoore, I. J. *et al.* Graphene–metamaterial photodetectors for integrated infrared sensing. *ACS Photonics* **3**(6), 936–941 (2016).
- Abeyasinghe, D. C. *et al.* Edge doping effect to the surface plasmon resonances in graphene nanoribbons. *J. Phys. Chem. C* **123**(32), 19820–19827 (2019).
- Emani, N. K. *et al.* Electrically tunable damping of plasmonic resonances with graphene. *Nano Lett.* **12**(10), 5202–5206 (2012).
- Fang, Z. *et al.* Active tunable absorption enhancement with graphene nanodisk arrays. *Nano Lett.* **14**(1), 299–304 (2014).
- Kim, Y. *et al.* Phase modulation with electrically tunable vanadium dioxide phase-change metasurfaces. *Nano Lett.* **19**(6), 3961–3968 (2019).
- Han, S. *et al.* Complete complex amplitude modulation with electronically tunable graphene plasmonic metamolecules. *ACS Nano* **14**(1), 1166–1175 (2020).
- Su, D. *et al.* Amplitude-phase modulation metasurface hologram with inverse angular spectrum diffraction theory. *J. Phys. D Appl. Phys.* **55**(23), 235102 (2022).
- Ren, Z. *et al.* Active and smart terahertz electro-optic modulator based on VO₂ structure. *ACS Appl. Mater. Interfaces.* **14**(23), 26923–26930 (2022).
- Forouzmand, A. & Mosallaei, H. Electro-optical amplitude and phase modulators based on tunable guided-mode resonance effect. *ACS Photonics* **6**(11), 2860–2869 (2019).
- Alexandros, E. *et al.* Atomic scale plasmonic switch. *Nano Lett.* **16**, 709–714 (2016).
- Agrawal, A. *et al.* An integrated electrochromic nanoplasmonic optical switch. *Nano Lett.* **11**, 2774–2778 (2011).
- Chakraborty, S. *et al.* Gain modulation by graphene plasmons in aperiodic lattice lasers. *Science* **351**(6270), 246–248 (2016).
- Low, T. & Avouris, P. Graphene plasmonics for terahertz to mid-infrared applications. *ACS Nano* **8**(2), 1086–1101 (2014).
- Wen, C. & Lanza, M. Calcium fluoride as high-k dielectric for 2D electronics. *Appl. Phys. Rev.* **8**(2), 021307 (2021).
- Huang, L. *et al.* Realization of mid-infrared broadband absorption in monolayer graphene based on strong coupling between graphene nanoribbons and metal tapered grooves. *Opt. Express* **26**(22), 29192–29202 (2018).
- Sarma, S. D. *et al.* Electronic transport in two-dimensional graphene. *Rev. Mod. Phys.* **83**(2), 407 (2011).
- Bao, Y. *et al.* Active control of graphene-based unidirectional surface plasmon launcher. *ACS Photonics* **2**(8), 1135–1140 (2015).
- Zhu, L. *et al.* Electrical control of terahertz polarization by graphene microstructure. *Opt. Commun.* **346**, 120–123 (2015).
- Hu, X. F. *et al.* A plasmon modulator by dynamically controlling the spatial distribution of carrier density in graphene. *Opt. Commun.* **513**, 128093 (2022).
- Bao, Q. & Loh, K. P. Graphene photonics, plasmonics, and broadband optoelectronic devices. *ACS Nano* **6**(5), 3677–3694 (2012).
- Alfarrozi, S. A. I. *et al.* Square wave quadrature amplitude modulation for visible light communication using image sensor. *IEEE Access* **7**, 94806–94821 (2019).

Author contributions

Xuefang Hu: Participation in the whole work; drafting of the article; Changgui Lu: model and design; Xiangyue Zhao: coding; Yinwei Gu: data analysis; Mengjia Lu: drafting of the article; Dechao Sun: final approval of the version to be published;

Funding

This work was supported in part by the National Natural Science Foundation of China (NSFC) (11874107).

Competing interests

The authors declare no competing interests.

Additional information

Correspondence and requests for materials should be addressed to X.H.

Reprints and permissions information is available at www.nature.com/reprints.

Publisher's note Springer Nature remains neutral with regard to jurisdictional claims in published maps and institutional affiliations.



Open Access This article is licensed under a Creative Commons Attribution 4.0 International License, which permits use, sharing, adaptation, distribution and reproduction in any medium or format, as long as you give appropriate credit to the original author(s) and the source, provide a link to the Creative Commons licence, and indicate if changes were made. The images or other third party material in this article are included in the article's Creative Commons licence, unless indicated otherwise in a credit line to the material. If material is not included in the article's Creative Commons licence and your intended use is not permitted by statutory regulation or exceeds the permitted use, you will need to obtain permission directly from the copyright holder. To view a copy of this licence, visit <http://creativecommons.org/licenses/by/4.0/>.

© The Author(s) 2023